scientific reports

Check for updates

OPEN

High sensitivity graphene based terahertz biosensor for accurate detection of blood antigens using a novel multilayer radial structure

Yousef Rafighirani, Hamid Heidarzadeh✉ & Javad Javidan

This study presents the design and development of an advanced graphene-based biosensor for the precise detection of blood antigens using three novel structural configurations. The sensor integrates graphene with localized surface plasmon resonance (LSPR) technology to achieve high sensitivity and selectivity in complex biological environments. The proposed structures consist of graphene layers, a silicon dioxide dielectric layer, and a gold base layer, further enhanced with gold nanoparticles. Simulation results indicate that the sensor achieves an absorption rate exceeding 98% in the terahertz regime, with the highest sensitivity reaching 10,514.1 GHz/RIU for the first structure, while the second and third structures exhibit sensitivities of 5,461.7 GHz/RIU and 2,390 GHz/RIU, respectively. The sensor reliably detects concentrations of hemoglobin (C_Hb) antigen ranging from 20 to 260 ng/mL with high precision. A key advantage is its polarization independence, ensuring stable performance regardless of the incident wave's polarization angle. Additionally, the sensor maintains high angular stability, operating effectively across incident angles from 0° to 60°. This graphene-based platform holds significant promise for the early detection of blood disorders, including anemia, thalassemia, and certain cancers. With its high diagnostic accuracy, real-time monitoring capabilities, and cost-effectiveness, it presents a viable alternative to traditional diagnostic techniques, advancing personalized medicine and point-of-care applications. To validate the proposed design method, RLC Equivalent circuit modeling is used, and there is a good agreement.

Keywords Biosensor, Graphene heterogeneous structure, Terahertz, Metamaterial, Reflectivity index

The ability to accurately and rapidly detect biomolecules is fundamental to modern medicine, particularly for disease diagnosis and management. Among these biomolecules, red blood cells (RBCs), which carry hemoglobin, play a crucial role in oxygen and carbon dioxide transport throughout the body. Any disruption in their function or structure can lead to severe health conditions, including anemia, sickle cell disease, and thalassemia. Therefore, developing highly sensitive and reliable detection methods for RBC-related biomarkers is essential for early diagnosis and effective treatment planning[1]. As the global burden of such disorders increases, the need for innovative, efficient, and precise diagnostic tools has never been more pressing. Recent advancements in biosensing technology have opened new pathways for identifying biological substances with unprecedented speed and accuracy. Leveraging breakthroughs in nanotechnology, biosensors have emerged as a game-changing solution, combining sensitivity with scalability[2]. In particular, graphene—a groundbreaking two-dimensional nanomaterial—has taken center stage due to its exceptional properties, including high electrical conductivity, a large surface area, and biocompatibility[3]. Combined with Localized Surface Plasmon Resonance (LSPR) technology, graphene-based biosensors present a transformative tool for biomedical diagnostics. Red blood cells serve as the body's oxygen couriers, enabling vital physiological processes. Monitoring RBCs is fundamental not only for diagnosing hematological disorders but also for tracking responses to treatments or therapies[4]. Conventional diagnostic methods, such as spectrophotometry or colorimetric assays, while reliable, have limitations. They often require complex equipment, and lengthy protocols and are highly sensitive to environmental interference[5]. These challenges emphasize the urgent need for advanced biosensors that provide accurate, real-time data with minimal operational complexity.

Department of Electrical and Computer Engineering, University of Mohaghegh Ardabili, Ardabil, Iran. ✉email: heidarzadeh@uma.ac.ir

Graphene's atomic-scale structure—just one layer of carbon atoms arranged in a honeycomb lattice—imbues it with unique physical and chemical characteristics. This material can detect minute biological interactions through subtle changes in its electrical or optical signals[6]. Unlike traditional sensing materials, graphene seamlessly interacts with biological molecules like antigens, proteins, and nucleic acids. Its biocompatibility ensures minimal interference with natural biological processes, making it a highly effective platform for biosensor development[7]. LSPR is a light-based phenomenon that occurs when metal nanoparticles interact with light, producing resonant oscillations of conduction electrons. These oscillations are highly sensitive to the molecular environment, allowing LSPR-based sensors to detect biomolecules without requiring chemical labels[8]. Integrating graphene with LSPR technology amplifies its sensitivity and mitigates common issues like molecular polarization, ensuring robust and reliable detection[9]. One of the most promising applications of graphene in biosensing lies in its integration with LSPR systems to detect red blood cells. This hybrid approach not only addresses challenges related to molecular alignment but also significantly enhances detection precision[10]. The graphene-LSPR combination allows for real-time, label-free monitoring of RBCs, paving the way for early diagnosis and effective management of blood disorders. Despite its immense potential, the journey to mainstream adoption of graphene-based biosensors faces hurdles. Manufacturing graphene at scale with consistent quality remains a challenge[11]. Additionally, the high cost of production and concerns over the long-term stability of nanomaterials hinder commercialization. Future efforts must focus on developing cost-effective fabrication techniques, improving the durability of these sensors, and exploring new materials to complement graphene's properties[12]. The integration of graphene and LSPR technology represents a quantum leap in diagnostic capabilities. By overcoming the limitations of traditional approaches, these sensors promise to revolutionize how we detect and monitor red blood cells and other biomolecules[13]. As research continues to refine this technology, its potential to transform healthcare is undeniable, offering faster, more reliable, and more accessible diagnostic tools. The future of medical diagnostics lies in harnessing the unique properties of materials like graphene. Its synergy with LSPR technology holds immense promise, not just for detecting red blood cells but for a broad spectrum of biomedical applications. With ongoing advancements in nanotechnology and material science, we are poised to enter a new era of precision medicine, where diseases are detected earlier and treated more effectively than ever before[14]. The time-difference gradient method (FDTD) is one of the powerful computational tools that is widely used to simulate and analyze the optical responses of nanostructures. Due to its capabilities in modeling complex electromagnetic interactions and its high accuracy, this method is used in various fields such as biosensing and optical communications. FDTD is particularly useful in studying the behavior of electromagnetic fields in real time and analyzing transient phenomena[15]. In addition, CST Studio Suite 2023 (Version 2023.01) on a Windows 10 64-bit system is used as an advanced simulation tool to calculate the absorption properties of the structures. This software uses the finite integration technique (FIT) to provide accurate and reliable simulations.

In this study, we explore the development of an ultra-sensitive graphene-based sensor designed for the detection of concentration of hemoglobin (C_Hb) antigens without polarization dependence. This sensor, utilizing a uniquely engineered structure of LSPR, demonstrates exceptional capability in detecting optical signals even in highly complex and challenging environments. The innovative design and fabrication methods of this sensor underscore its potential to revolutionize the analysis of biological samples and pave the way for significant advancements in medical diagnostic technologies.

Graphene has emerged as a transformative material in terahertz technology due to its unique properties. For instance, graphene's exceptional electrical, mechanical, and optical characteristics, combined with the versatile functionality of metamaterials and metasurfaces, have led to the development of highly efficient and dynamic lens systems[16]. Moreover, by adjusting the graphene's chemical potential, terahertz sensors can achieve tunability, enabling precise control over their electromagnetic response for environmental and biosensing applications[17]. These advancements underscore the potential of graphene in terahertz biosensing, inspiring our design of a novel multilayer architecture with a radial pattern for ultra-high-sensitivity blood antigen detection.

The architecture of this sensor integrates graphene, a material renowned for its extraordinary electrical, optical, and mechanical properties, with an optimized LSPR structure. This combination enables the sensor to achieve high sensitivity and selectivity, even in the presence of noise or environmental interference. Unlike traditional sensors, this design eliminates polarization dependence, ensuring consistent performance regardless of the orientation of the target molecules. The ability to detect C_Hb antigens with exceptional sensitivity has profound implications for medical diagnostics. For instance, this technology can be beneficial in the early detection of blood-related disorders such as anemia, thalassemia, and even certain types of cancer. Furthermore, the sensor's real-time monitoring capabilities could enhance the tracking of therapeutic responses, providing a more personalized approach to patient care. The innovative techniques used in the construction of this sensor, alongside its demonstrated capabilities, position it as a transformative tool in the field of biosensing. Future research could focus on scaling production, improving cost-effectiveness, and exploring additional applications in areas such as environmental monitoring and food safety. The findings of this research emphasize the potential of graphene-based sensors for significant advancements in diagnostic technologies. With the capability for early detection and precise monitoring of diseases, this technology could play a crucial role in improving patient outcomes, particularly for cancer patients. As we refine and expand such sensors' capabilities, we move closer to a future where advanced diagnostics become more accessible, accurate, and impactful. This study introduces a novel biosensor that offers faster and more reliable blood antigen detection compared to traditional methods. A key innovation of this design is its ability to regulate absorption frequency based on specific clinical needs, significantly reducing diagnostic time and costs without compromising accuracy. Additionally, the sensor overcomes common challenges, such as chemical and biological instability and signal disturbances, which have limited the effectiveness of previous approaches. By enabling customizable absorption frequencies, the proposed biosensor enhances versatility across diverse diagnostic applications. Its ability to deliver rapid and cost-effective results holds significant potential for improving patient outcomes by facilitating quicker clinical decision-making and intervention. Furthermore, its enhanced stability and robustness ensure more reliable detection, positioning it as a promising alternative to conventional diagnostic technologies.

Simulation methodology and design

Graphene, a two-dimensional material with remarkable semi-conducting properties, has emerged as a game-changer in the field of plasmonics. Its unique characteristics, such as bidirectional performance and exceptional tunability, make it an ideal candidate for a wide range of applications. By integrating graphene into plasmonic structures, researchers can significantly enhance performance while unlocking new opportunities for innovation in fields such as sensing, imaging, and telecommunications[18]. The conductivity of graphene in the terahertz (THz) range is a critical factor in its performance and is determined by a set of equations. Equation (1) describes the total conductivity of graphene, which is derived from the sum of intra-band and inter-band conductivity contributions. Equation (2) specifically calculates the inter-band conductivity, while Eq. (3) is used to determine the intra-band conductivity. These equations provide a comprehensive framework for understanding and optimizing graphene's electrical properties in plasmonic applications[19].

$$\sigma\left(\omega, \tau, \mu_c, T\right) = \sigma_{\text{int}\,er}\left(\omega, \tau, \mu_c, T\right) + \sigma_{\text{int}\,era}\left(\omega, \tau, \mu_c, T\right) \tag{1}$$

$$\sigma_{\text{int}\,er}\left(\omega, \tau, \mu_c, T\right) = -j\frac{e^2}{4\pi\hbar}\ln\left(\frac{2\mu_c + (\omega - j\tau^{-1})\hbar}{2\mu_c - (\omega - j\tau^{-1})\hbar}\right) \tag{2}$$

$$\sigma_{\ \text{int}\,era}\left(\omega\ ,\ \tau,\ \mu_c,\ T\right) = -j\frac{e^2\ K_B\ T}{\pi\ \hbar^2\ \left(\omega\ -j\ \tau^{-1}\right)}\left[\frac{\mu_c}{K_B\ T} + 2\ \ln\left(\exp\ \left(-\frac{\mu_c}{K_B\ T}\right) + 1\right)\right] \tag{3}$$

In the above equations, ω, angular frequency, τ, relaxation time, chemical potential of graphene, T, temperature in Kelvin (in this article, the value of T = 300k) e, electrical chargeK_B Boltzmann's constant, ħ Planck's reduced constant are defined. According to Pauli's exclusion principle, since it is $\mu_c \gg K_B T$ in terahertz in the infrared band, the inter-band part in graphene can be ignored and the conductivity can be summarized as follows:

$$\sigma\left(\omega, \tau, \mu_c\right) = \frac{je^2\mu_c}{\pi\hbar^2(\omega + j\tau^{-1})} \tag{4}$$

One of graphene's most notable features is its ability to exhibit bidirectional performance, meaning it can efficiently interact with electromagnetic waves in multiple directions. Combined with its extensive tunability, this property allows graphene to be tailored for specific applications. For instance, by adjusting parameters such as doping levels or external electric fields, researchers can fine-tune graphene's optical and electrical responses to meet the demands of advanced plasmonic devices. The integration of graphene into plasmonic structures has far-reaching implications. In sensing, graphene-enhanced plasmonic devices can achieve ultra-high sensitivity, enabling the detection of minute quantities of biological or chemical substances. Graphene's tunability and conductivity can improve resolution and contrast in imaging, making it invaluable for medical diagnostics and security screening. In telecommunications, graphene-based plasmonic components can facilitate faster and more efficient data transmission, paving the way for next-generation communication networks.

Biosensor design using the proposed structure

Impedance is a key concept in electrical engineering and physics that refers to the resistance of a system to electric current or electromagnetic waves. In the field of electromagnetic waves, impedance describes how a material or structure responds to electric and magnetic fields. The impedance of free space (Z_0) is a constant value and is approximately equal to 377 ohms. This value is used as a reference to compare the impedance of other materials.

When electromagnetic waves are transmitted from one medium to another medium with different impedances, part of the wave energy may be reflected. This reflection phenomenon occurs when the impedance difference between two environments is significant. To reduce this reflection and increase energy absorption, impedance matching is necessary. In this case, the impedance of the structure or material is adjusted to be as close as possible to the impedance of free space[20]. In applications such as designing antennas, solar cells, and wave-absorbing materials, impedance matching plays a vital role. For example, by using materials such as graphene that have tunable electrical and optical properties, the effective impedance of the structure can be precisely controlled. This adjustability allows for almost complete absorption of electromagnetic waves and minimizes reflections. In this way, impedance matching is not only a theoretical concept but also a practical tool to improve the performance of electromagnetic systems.

For practical implementation of the proposed terahertz biosensor, specific environmental conditions are required to ensure reliable performance. The sensor should be operated at a stable temperature of 20–37 °C to preserve the electrical properties of graphene and the stability of gold nanoparticles and to avoid degradation due to extreme heat or cold. The relative humidity should be controlled between 30 and 60%, controllable in water. With the recommended encapsulation in humid conditions, electromagnetic interference should be minimized (e.g., through shielding) to maintain the accuracy of terahertz signal detection and selectivity in real-world applications.

Proposed structure with the graphene layer

As shown in Fig. 1(a), the unit cell of the proposed full periodic absorber structure is carefully fabricated to optimize performance. Figure 1(b) provides a close-up view of the structure, which consists of a graphene layer with special properties, a dielectric layer, and a conductive base layer. Several key features define the graphene layer in this design: it has a relaxation time of 2 ps, a thickness of 1 nm, a chemical potential of 0.4 eV, and operates at a temperature of 300 K. This graphene layer has a triangular cut on the sides, the size of the base side of each triangle is 0.5 µm and the graphene disk with a radius of 0.3 µm is strategically arranged to increase the absorption capabilities of the structure. Under the graphene layer, there is a dielectric layer made of silicon dioxide (SiO2), which is characterized by a relative permittivity of 3.9[18] and a thickness of 4.2 µm. This layer of silicon dioxide acts as a support layer for the graphene layer and contributes to the overall optical and electrical performance of the structure. The bottom layer is made of gold, a highly conductive metal with a conductivity of 4.7×10^7 S/m[18] and a thickness of 0.3 µm. The gold layer acts as a reflective surface, ensuring that incident electromagnetic waves are effectively absorbed rather than transmitted. A width of 2.5 µm defines the overall dimensions of the unit cell, and the structure is arranged periodically in the x and y directions, with open boundary conditions applied in the z direction to simulate an infinite structure. According to electromagnetic field theory, the absorption value A(ω) of the structure is expressed by Eq. 5, where R(ω) denotes the reflectance and T(ω) represents the transmittance. This equation quantifies the structure's capacity to absorb incident electromagnetic waves, serving as a crucial metric for assessing its performance.

$$A(\omega) = 1 - R(\omega) - T(\omega) = 1 - |s_{11}(\omega)|^2 - |s_{21}(\omega)|^2 \quad (5)$$

In conclusion, the proposed graphene-based full absorber structure, with its thoughtfully engineered layers and periodic configuration, shows significant promise for applications in photonics, sensing, and energy harvesting. By harnessing the unique properties of graphene, silicon dioxide, and gold, this structure achieves high absorption efficiency, paving the way for advancements in optical and plasmonic technologies. The absorption curves of the proposed structure were drawn in Fig. 2(a) by changing the relaxation time of graphene from 2ps, 3ps, and 4ps. Figure 2(b) plots it as the chemical potential changes from 0.4 eV, 0.5 eV, and 0.6 eV. The absorption curve shown in Fig. 2(c) corresponds to the refractive index of C_Hb analyte with different concentrations used in Table 1. Graphene enhances electromagnetic wave absorption by adjusting the structure's impedance to match free space (377 Ω), minimizing reflection. Its tunable conductivity, controlled by chemical potential, plays a key role. As shown in Fig. 2(b), absorption peaks at 0.97(97%) for $\mu_c = 0.4$ eV around 4.5 THz, compared to 0.85(85%) at 0.5 eV and 0.7(70%) at 0.6 eV, indicating optimal impedance matching at 0.4 eV. Gold nanoparticles further boost absorption via LSPR, concentrating the field near graphene. This demonstrates graphene's critical role in achieving high absorption and sensitivity in the terahertz biosensor.

We analyzed the refractive index at different concentrations of hemoglobin to understand how the sensor behaves. After this analysis, we simulated the sensor's structure under similar conditions. This allowed us to calculate the sensor's sensitivity by examining the change in its resonance frequency as the refractive index changed.

$$S = \frac{\Delta f}{\Delta n} \quad (6)$$

Moreover, the figure of merit (FOM) is defined as:

$$FOM = \frac{S}{FWHM} \quad (7)$$

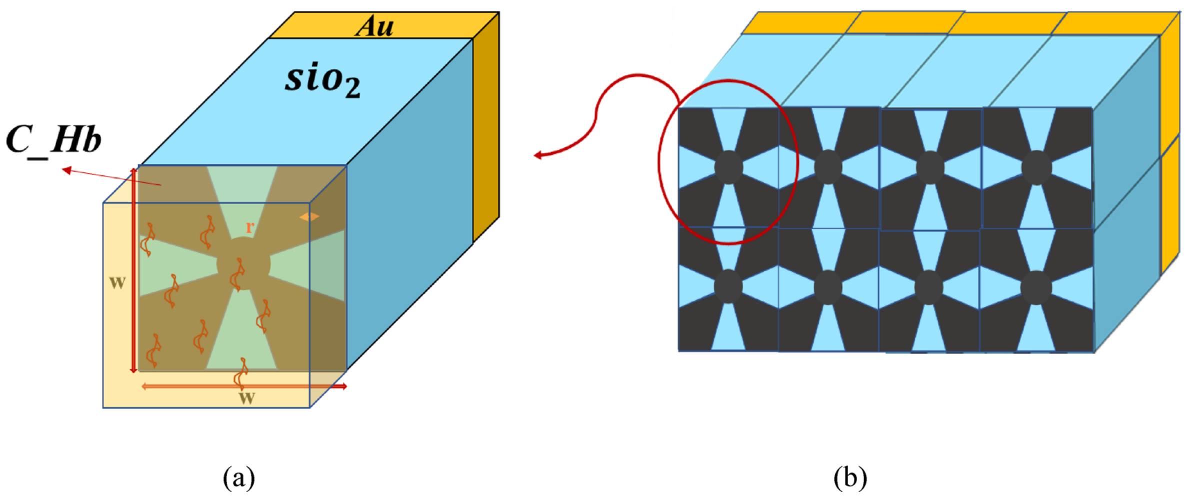

Fig. 1. **(a)** A cell of the periodic structure **(b)** Complete structure of a complete absorber.

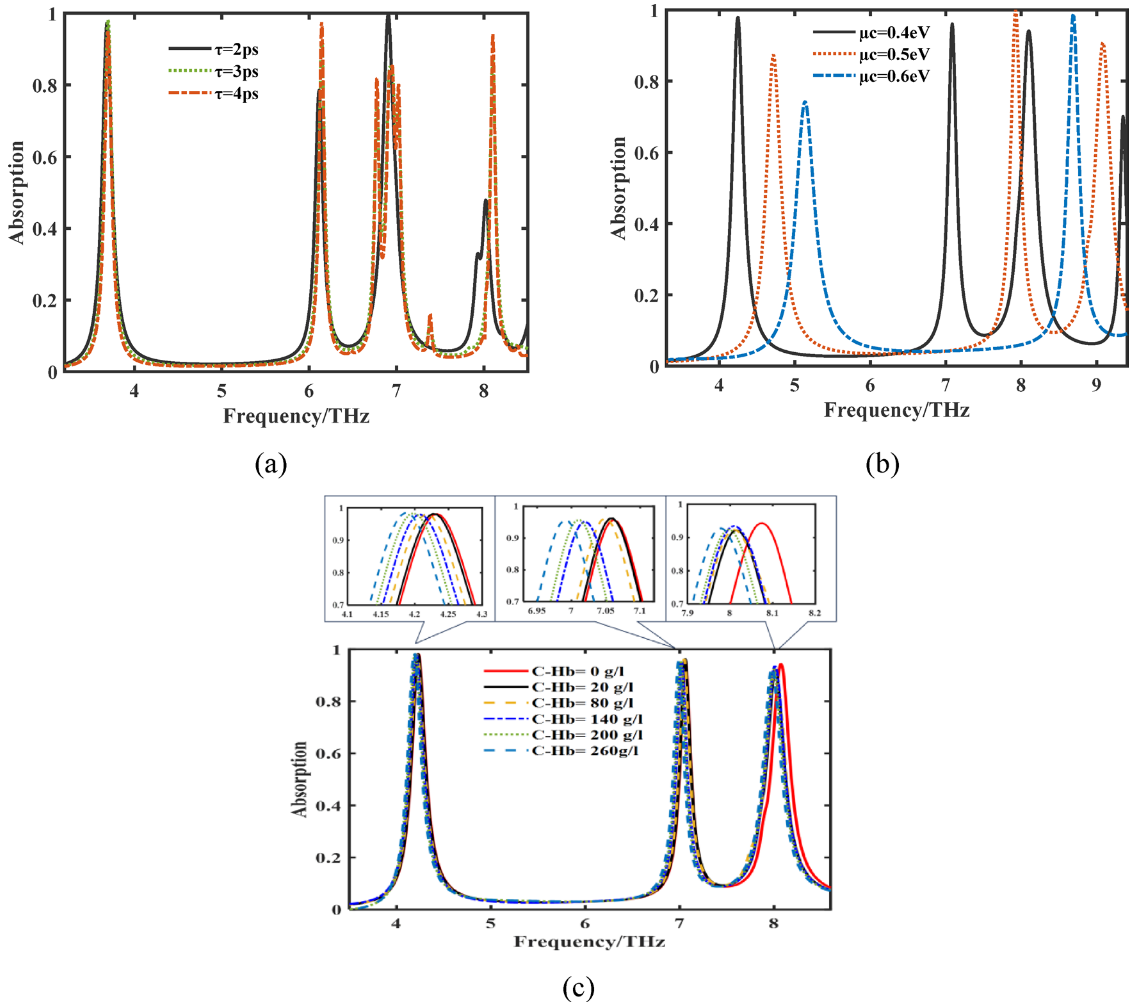

Fig. 2. **(a)** varying relaxation time of graphene from 2ps, 3ps, and 4ps. **(b)** varying chemical potential changes from 0.4 eV, 0.5 eV, and 0.6eV **(c)** related to the refractive index of hemoglobin the analyte with different concentrations.

C_Hb (g/l)	$n = n0 + \Delta n$
0	$n = 1.33$
20	$n = 1.335859$
80	$n = 1.351588$
140	$n = 1.367316$
200	$n = 1.383044$
260	$n = 1.398773$

Table 1. The corresponding refractive index of hemoglobin in different concentrations ($n_0 = 1.33$)[21].

Table 2 shows five different concentrations of hemoglobin antigen with a refractive index between 1.335859 and 1.398773 in the analyte layer. Then, these samples are simulated, and their absorption spectra are plotted and shown in Fig. 2(c). A detailed examination of Table 2, derived from the absorption curve illustrated in Fig. 2 (c), indicates that the amount of absorption at all analyte concentrations exceeds 98%, signifying complete absorption. A careful analysis of Table 2, based on the absorption curve presented in Fig. 2 (c), reveals that the curve comprises three distinct bands, each displaying varying sensitivity of the analyte at different concentrations, which are represented through varying refractive indices in Table 2. The highest sensitivity is observed in the first band, at 1194.7 GHz/RIU.

The FOM was calculated using the formula provided in the study, yielding a value of 6.9 for the first band. The limit of detection (LOD), which indicates the minimum detectable concentration of the analyte in a sample, was computed using the formula LOD = Fr/(20) × S×Q[22]. The lowest detected value is 0.007, while in the second

Refractive index	First band				Second band				Third band			
	Freq (THz)	S (GHz/RIU)	FOM	LOD	Freq (THz)	S (GHz/RIU)	FOM	LOD	Freq (THz)	S (GHz/RIU)	FOM	LOD
$n = 1.33$	4.233	—	—	—	7.061	—	—	—	8.076	—	—	—
$n = 1.335859$	4.226	1194.7	6.9	0.007	7.055	946.2	7.1	0.007	8.014	10514.1	55.9	0.0009
$n = 1.351588$	4.215	833.8	4.8	0.01	7.049	558.6	4.2	0.012	8.009	3074.3	16.4	0.0031
$n = 1.367316$	4.205	750.3	4.3	0.012	7.019	1127.1	8.5	0.006	8.009	1778.9	9.5	0.0053
$n = 1.383044$	4.196	697.5	4	0.012	7.009	986.6	7.4	0.007	7.997	1476.4	7.9	0.0064
$n = 1.398773$	4.184	712	4.1	0.012	6.989	946	7.9	0.006	7.976	1436.4	7.6	0.006

Table 2. The results derived from the variations in the refractive index of the analyte layer corresponding to different concentrations of hemoglobin are presented.

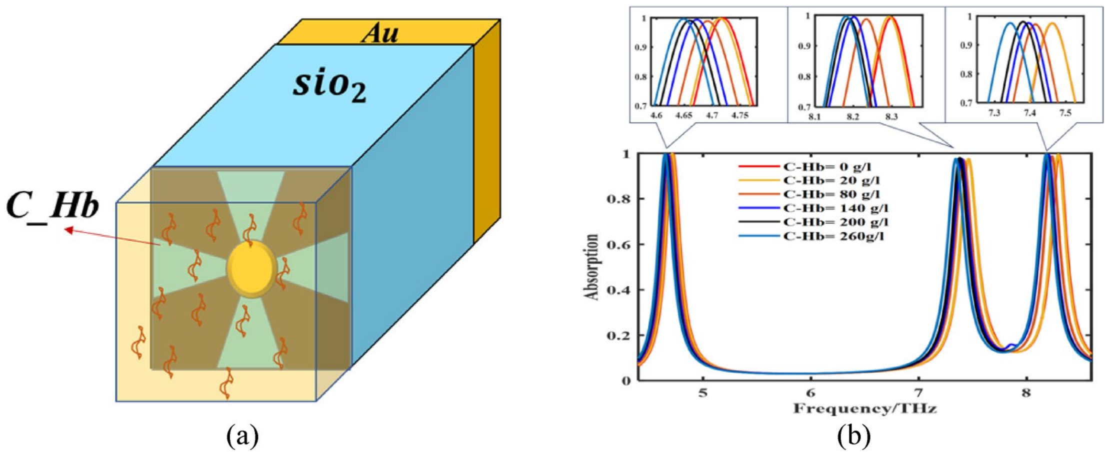

Fig. 3. **(a)** A cell of the periodic structure **(b)** related to the refractive index of the hemoglobin analyte with different concentrations.

band, the highest sensitivity measured is 1127 GHz/RIU. The FOM for this band is calculated as 8.5, with a LOD of 0.006. In the third band, the peak sensitivity reaches 10,514 GHz/RIU, resulting in a FOM of 55.9 and a LOD of 0.0009.

Proposed structure with graphene layer and gold nanoparticles in the center

The frequency-absorbing structure designed for use in a biosensor based on graphene and gold nanoparticles represents an innovative approach to enhancing sensitivity and selectivity in the detection of biomolecules. The graphene layer serves as the sensitive component, providing improved interaction with target molecules due to its tunable electronic properties and high surface-to-volume ratio. Gold nanoparticles, which can be dispersed or patterned on the graphene, enhance local electromagnetic fields through plasmonic effects, creating suitable binding sites for biomolecules. This design offers high sensitivity due to the amplification of electromagnetic fields and supports use in compact and multifunctional devices, thanks to the tunable properties of graphene and its compact design. As depicted in Fig. 3 (a), the gold nanoparticle with a radius of 0.3 micrometers and a thickness of 0.2 micrometers is positioned at the center of the structure, where all material information and dimensions correspond to those of the initially designed structure shown in Fig. 3 (a). The only difference lies in the placement of the gold nanoparticles. The absorption curve of the graphene structure combined with the gold nanoparticle for various concentrations of hemoglobin is illustrated in Fig. 3 (b).

A detailed examination of Table 3, derived from the absorption curve illustrated in Fig. 3 (b), reveals that the absorption rate at all analyte concentrations exceeds 98%, indicating complete absorption. A thorough analysis of Table 3, based on the absorption curve presented in Fig. 3 (b), shows that the curve comprises three distinct bands, each demonstrating the variable sensitivity of the analyte at different concentrations, represented through variable refractive indices in Table 3. The highest sensitivity is observed in the first band, at 1414.2 GHz/RIU. The FOM was calculated using the formula provided in the study, yielding a value of 8.7 for the first band. The LOD, which indicates the minimum detectable concentration of the analyte in a sample, is found to be 0.006. In the second band, the highest measured sensitivity is 5461 GHz/RIU, with a FOM of 33.5 and a LOD of 0.001. In the third band, peak sensitivity reaches 3242 GHz/RIU, resulting in a FOM of 17.2 and a LOD of 0.003.

Refractive index	First band				Second band				Third band			
	Freq (THz)	S (GHz/RIU)	FOM	LOD	Freq (THz)	S (GHz/RIU)	FOM	LOD	Freq (THz)	S (GHz/RIU)	FOM	LOD
n = 1.33	4.721	—	—	—	7.472	—	—	—	8.301	—	—	—
n = 1.335859	4.713	1305.7	8	0.006	7.44	5461.7	33.5	0.001	8.29	1877.5	10	0.005
n = 1.351588	4.69	1414.2	8.7	0.006	7.411	2825.6	17.3	0.003	8.231	3242.5	17.2	0.003
n = 1.367316	4.671	1338.6	8.2	0.006	7.391	2170.7	13.3	0.004	8.197	2787	14.8	0.003
n = 1.383044	4.658	1183	7.3	0.007	7.372	1885.2	11.6	0.004	8.185	2186.9	11.6	0.004
n = 1.398773	4.648	1054	6.5	0.008	7.331	2050.2	12.5	0.004	8.175	1820.4	9.6	0.005

Table 3. The results derived from the variations in the refractive index of the analyte layer corresponding to different concentrations of hemoglobin are presented.

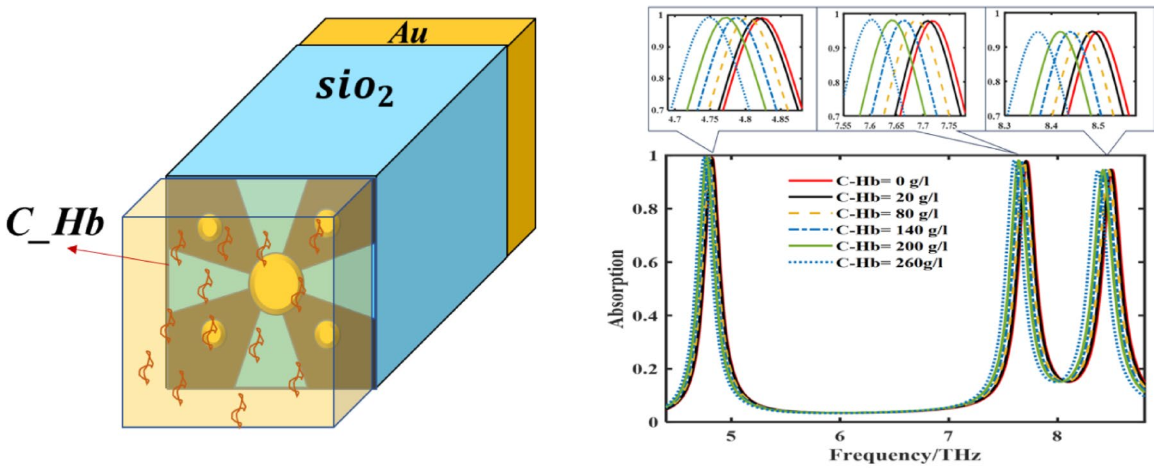

(a) (b)

Fig. 4. **(a)** A cell of the periodic structure **(b)** related to the refractive index of the C_Hb analyte with different concentrations.

Refractive index	First band				Second band				Third band			
	Freq (THz)	S (GHz/RIU)	FOM	LOD	Freq (THz)	S (GHz/RIU)	FOM	LOD	Freq (THz)	S (GHz/RIU)	FOM	LOD
n = 1.33	4.825	—	—	—	7.723	—	—	—	8.5	—	—	—
n = 1.335859	4.816	1536	8.9	0.006	7.709	2389	13.8	0.005	8.486	2390	13.8	0.005
n = 1.351588	4.801	1112	6.4	0.008	7.687	1668	9.6	0.005	8.464	1669	9.6	0.005
n = 1.367316	4.785	1072	6.2	0.008	7.66	1688	9.8	0.005	8.437	1688	9.8	0.005
n = 1.383044	4.767	1093	6.3	0.008	7.637	1621	9.4	0.005	8.415	1602	9.3	0.004
n = 1.398773	4.745	1163	6.7	0.007	7.597	1832	10.6	0.005	8.367	1933	11.2	0.004

Table 4. The results derived from the variations in the refractive index of the analyte layer corresponding to different concentrations of hemoglobin are presented.

Proposed structure with graphene layer and gold nanoparticles in the center and surrounding

The third frequency-absorbing structure designed for use in graphene-based biosensors, as illustrated in Fig. 4 (a), is distinguished by the addition of four gold nanoparticles with a radius of 0.1 micrometers and a thickness of 0.2 micrometers, positioned on a graphene branch. A detailed examination of Table 4, derived from the absorption curve illustrated in Fig. 4 (b), reveals that the absorption rate at all analyte concentrations exceeds 98%. A thorough analysis of Table 4, based on the absorption curve presented in Fig. 3 (b), shows that the curve comprises three distinct bands, each demonstrating the variable sensitivity of the analyte at different concentrations, represented through variable refractive indices in Table 4.

The highest sensitivity is observed in the first band, at 1536 GHz/RIU. The FOM was calculated using the formula provided in the study, yielding a value of 8.9 for the first band. The LOD, which indicates the minimum detectable concentration of the analyte in a sample, is found to be 0.006. In the second band, the highest measured sensitivity is 2389 GHz/RIU, with a FOM of 13.8 and a LOD of 0.005. In the third band, peak sensitivity reaches 2389 GHz/RIU, resulting in a FOM of 13.8 and a LOD of 0.004.

By carefully examining Table 5, the results obtained are as follows. The proposed structure in this study is compared with previous works in terms of design, sensitivity, fom, and analyte. The proposed structure demonstrates superior sensitivity compared to previous designs, such as the "Four-Trishel" structure (196 GHz/RIU) with an FoM of 19.65, the "Two-Layer graphene disc" (1100 GHz/RIU) with a FoM of 12.5, the "Semi-Circular graphene rings" (1400 GHz/RIU) with a FoM of 17.3, and the "Five-Segment" structure (2660 GHz/RIU) with a FoM of 26.6. Recent studies further highlight the competitive performance of our design. The "Dual-band polarization-independent maze-shaped absorber" achieves a sensitivity of 1150 ghz/riu with an FoM of 1.55, the "terahertz plasmonic biosensor leveraging Ag-Au-Graphene" reports 1000 ghz/riu with an FoM of 3.289, and the "sensitivity increment of metamaterial-based sensor with silicon layers" offers 5764 ghz/riu with an FoM of 21.34. The sensitivity of the first designed structure is significantly greater at 10514.1 ghz/riu, with an FoM of 55.9, in comparison to all these designs. Additionally, the second structure exhibits a sensitivity of 5461.7 ghz/riu and a FoM of 33.5, while the third structure shows a sensitivity of 2390 ghz/riu and a FoM of 13.8, which indicates better performance than most other designs and highlights its superior capability in detecting the analyte. This study focuses on the detection of c_hb, achieving improved accuracy. These results emphasize the effectiveness of the proposed design for biosensing applications, surpassing the limitations of prior works.

Sensitivity and FoM Comparison Across Three Bands for Different Structures. Figure 5 illustrates the sensitivity (solid lines, left y-axis) and FoM (dashed lines, right y-axis) of three structures as a function of the refractive index (blue: Structure 1, red: Structure 2, green: Structure 3) across three frequency bands. Figure 5(a) illustrates the First Band (around 4.2 to 4.8 THz), Structure 3 exhibits the highest sensitivity, ranging from 1536 to 1163 GHz/RIU, and FoM from 8.9 to 6.7 RIU^{-1}, followed by Structure 2 with sensitivity from 1305.7 to 1054 GHz/RIU and FoM from 8 to 6.5 RIU^{-1}, while Structure 1 shows the lowest sensitivity, ranging from 1194.7 to 712 GHz/RIU, and FoM from 6.9 to 4.1 RIU^{-1}. Figure 5(b) illustrates the Second Band (around 7.0 to 7.7 THz), Structure 2 demonstrates the highest sensitivity, peaking at 5461.7 GHz/RIU and decreasing to 2050 GHz/RIU, with FoM from 33.5 to 12.5 RIU^{-1}, followed by Structure 3 with sensitivity from 2389 to 1832 GHz/RIU and FoM from 13.8 to 10.6 RIU^{-1}, while Structure 1 has the lowest sensitivity, ranging from 946.2 to 946 GHz/RIU, and FoM from 7.1 to 7.9 RIU^{-1}. Figure 5(c) illustrates the Third Band (around 8.0 to 8.5 THz), Structure 1 shows exceptional sensitivity, peaking at 10514.1 GHz/RIU and decreasing to 1436.4 GHz/RIU, with FoM from 55.9 to 7.6 RIU^{-1}, followed by Structure 2 with sensitivity from 3242.5 to 1820.4 GHz/RIU and FoM from 17.2 to 9.6 RIU^{-1}, while Structure 3 has sensitivity from 2390 to 1933 GHz/RIU and FoM from 13.8 to 11.2 RIU^{-1}. Overall, each structure excels in a specific band, with Structure 3 dominating the First Band, Structure 2 the Second Band, and Structure 1 the Third Band, highlighting their suitability for different frequency ranges.

Independent of polarization

Figure 6 (a) shows that the resonance peak value remains consistent despite varying the polarization angle between 0°, 30°, 60°, 90°, and 120°. This indicates that the shape of the diagram remains unchanged across these three polarization angles, suggesting that the biosensor structure is polarization-independent. This characteristic is beneficial as it enhances the practicality and suitability of the biosensor for detecting specific analytes. So, the biosensor's performance remains stable and reliable regardless of the polarization angle used, which is advantageous for its application in analytical tasks such as detecting desired analytes. Figure 6(b) illustrates a magnetic wave with oblique radiation that influences both the absorption characteristics and the angular stability capability. These features are analyzed across a range of angles, depending on the value of θ, at which the absorber exhibits nearly constant characteristics. Consequently, the proposed terahertz absorber demonstrates remarkable stability against variations in the angle of incidence from 0 to 60 degrees. Given the inherent polarization of the terahertz absorber, its behavior remains non-sensitive and similar for both TM (Transverse Magnetic) and TE (Transverse Electric) modes of propagation. Therefore, it can be concluded that

Design		Sensitivity (GHz/RIU)	FoM	Analyte
Four Trishul structures with a cross-aperture[23]		196	19.65	Refractive Index
Two-layer graphene disk[24]		1100	12.5	Breast Cancer
Graphene semicircle rings[25]		1400	17.3	Refractive Index
Five-segment[26]		1440	26.6	CEA
Dual-band polarization-independent maze-shaped[27]		1150	1.55	Biomedical
Terahertz Plasmonic Biosensor Leveraging Ag-Au-Graphene[28]		1000	3.289	Hemoglobin
Sensitivity increment of metamaterial-based[29]		5764	21.34	Refractive Index
This work	The first structure	10514.1	55.9	C_Hb
	The second structure	5461.7	33.5	
	The third structure	2390	13.8	

Table 5. Comparing the results of the proposed structure with the results of previous works.

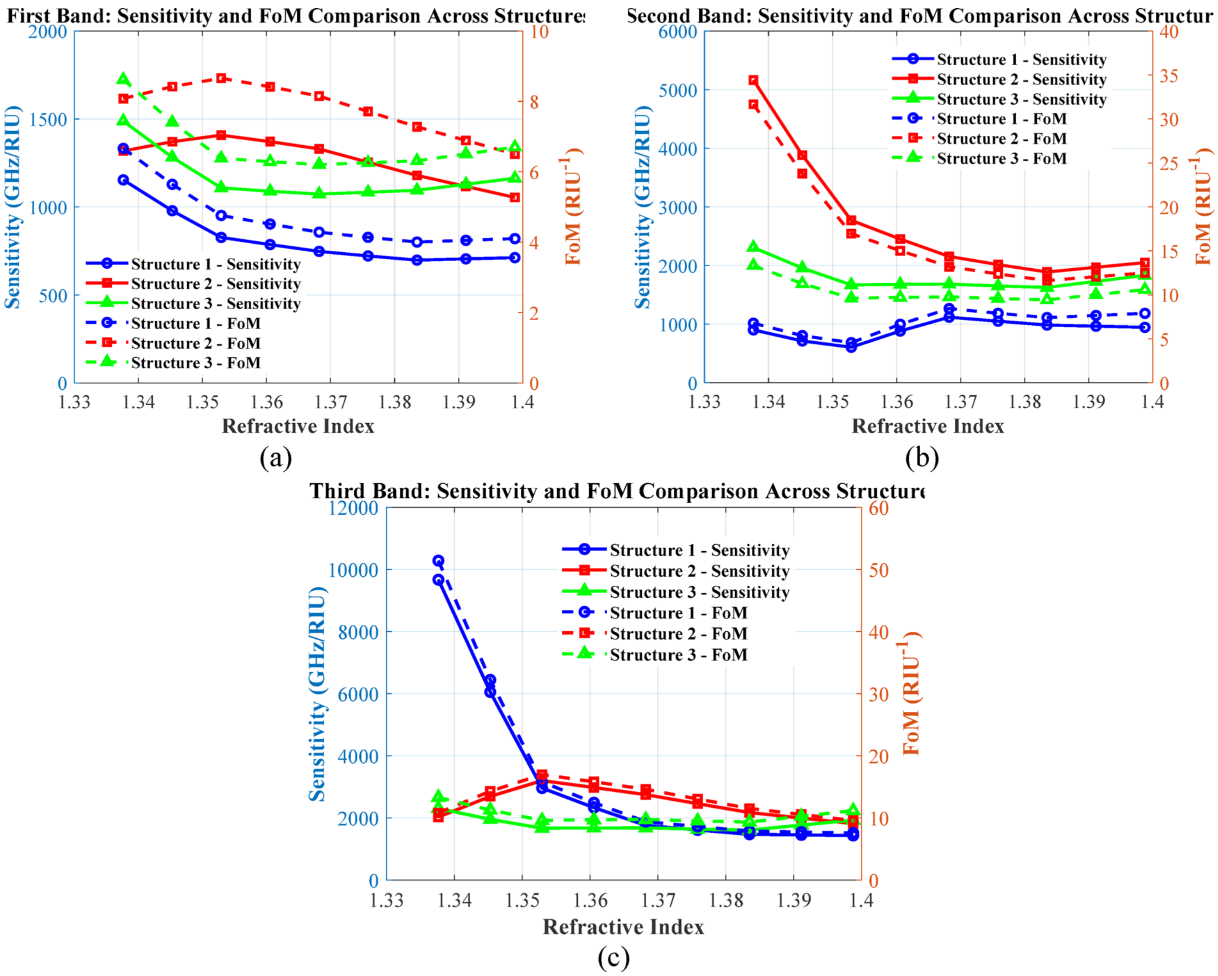

Fig. 5. Sensitivity (solid lines, left y-axis) and FoM (dashed lines, right y-axis) of the three structures across the **(a)** First, **(b)** Second, and **(c)** Third Bands as a function of refractive index.

the proposed absorber maintains high stability against changes in the incoming radiation's angle and intensity. This claim is due to the structural symmetry and properties of the materials. The radial pattern eliminates directional dependence and makes the response uniform for both transverse magnetic (TM) and transverse electrical (TE) modes. This was confirmed by the FDTD simulation, which the image of Figure. 6(c) shows this issue.

Analysis and design of equivalent circuit for frequency absorber

This section focuses on analyzing and designing an equivalent circuit for a frequency absorber. Initially, the overall structure of the equivalent circuit and its components are introduced. Following this, the frequency absorption graph of the circuit is presented, illustrating its performance within the desired frequency range. Subsequently, the mathematical equations relevant to calculating input impedance, wave propagation coefficient, and other important parameters of the circuit are provided. These equations enable the precise calculation of resistance, inductance, and capacitance values within the structure. The goal of this analysis is to optimize the performance of the frequency absorber by utilizing the unique properties of graphene layers.

The equivalent circuit with lumped elements for the absorber is designed and shown in Fig. 7. The substrate is modeled with a short circuit with impedance zero, which in this proposed structure is made of copper. A connecting line with impedance $Z_{TL}$and electrical length$E_{TL} = 2 \times \beta_{TL} \times T_S$ is used to model SiO_2. Each graphene layer can be modeled as a combination of resistive (R), capacitive (C), and inductive (L) components in parallel. The total input impedance (Z_{in}) of the network can be found by combining the impedances of all branches. The free space impedance is given as 377 Ω (or 120π Ω). When calculating the input impedance relative to free space, you might consider matching conditions that can affect R, L, and C values to optimize performance[29]:

$$Z_1 = jZ_{TL}\tan(\beta_{TL}T_s) \tag{8}$$

$$\beta_{TL} = 2\pi f\sqrt{\varepsilon_0\varepsilon_r\mu_0} \tag{9}$$

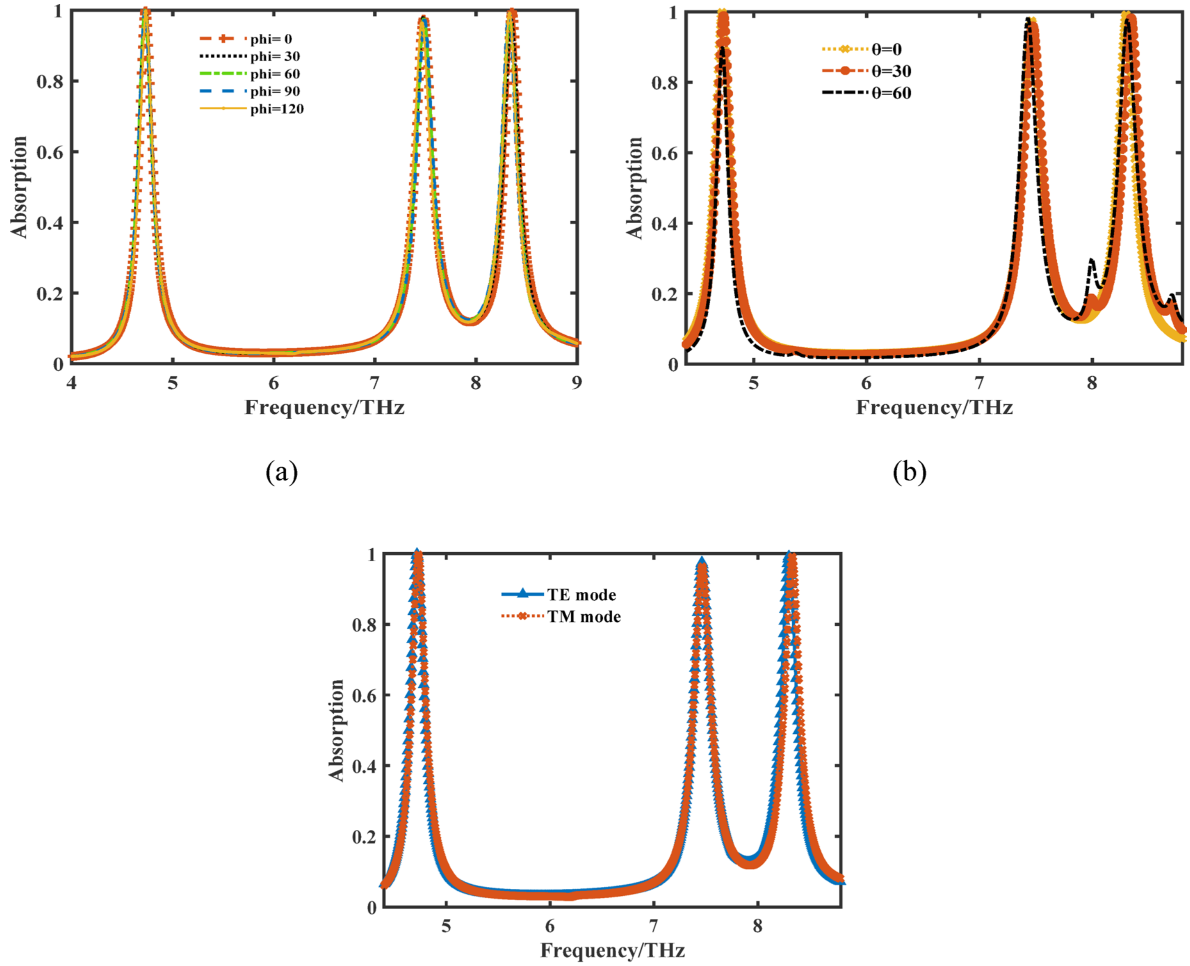

(a) (b) (c)

Fig. 6. **(a)** Absorption curve with three different polarization angles. **(b)** output frequency spectrum for different values of radiation angle. **(c)** Terahertz sensor absorption spectrum for TE and TM modes.

$$Z_{TL} = \sqrt{\mu_0/\varepsilon_0\varepsilon_r} \tag{10}$$

$$Z_G(f) = R + jX_G = R + j(2\pi fL - \frac{1}{2\pi fC}) = \frac{1}{\sigma_g(f)} \tag{11}$$

$$Z_{in} = \frac{Z_1.Z_g}{Z_1 + Z_g} \tag{12}$$

Where β_{TL} and ε_r represent the wave number and relative permittivity of the dielectric, respectively. Additionally, the following equations can be utilized to calculate the values of resistance (R), inductance (L), and capacitance (C) in a structure consisting of graphene layers. These equations are related to various factors, including the magnetic permeability (μr) and the relative permittivity (εr)[30]:

$$R = \frac{KL^2}{\pi S^2}\frac{\hbar^2}{e^3\mu_c\tau},\ L = \frac{KL^2}{\pi S^2}\frac{\hbar^2}{e^3\mu_c},\ C = \frac{\pi^2 S^2}{L^2 k}\frac{\varepsilon}{q_1} \tag{13}$$

Fabrication process of a gold graphene structure with nanoparticles

The conductive layer, composed of gold for this simulation, is located at the bottom of the structure. Following this, a dielectric layer made of silicon oxide is deposited on top of the gold layer using the physical vapor deposition (PVD) technique. Subsequently, a graphene layer is applied onto the silicon oxide via the chemical vapor deposition (CVD) method. Photolithography is then employed to etch patterns into the graphene, achieving the desired structural design. In the next step, gold nanoparticles are deposited onto the graphene layer using the CVD technique, with their thickness carefully controlled through a monitoring technique. This entire fabrication process results in the overall structure illustrated in Fig. 8.

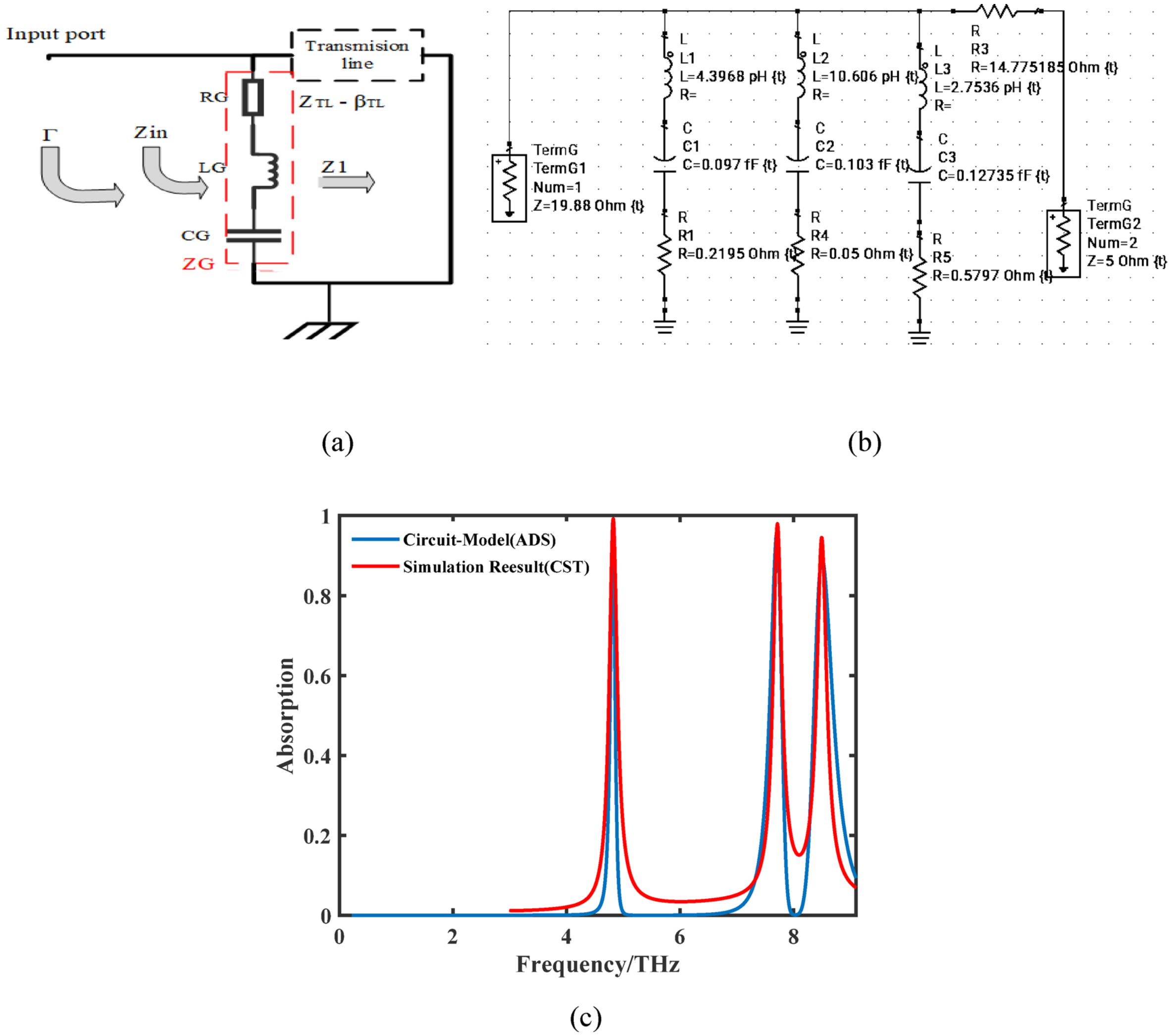

Fig. 7. **(a)** The general scheme of the equivalent circuit of the frequency absorber **(b)** the equivalent circuit of the absorber structure is designed by ADS **(c)** the absorption curve of the circuit model and simulation.

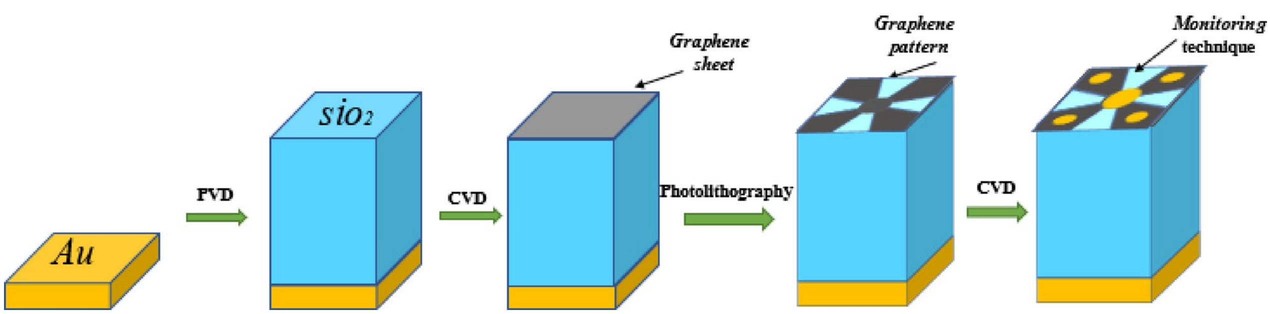

Fig. 8. The fabrication procedure for the proposed metamaterial absorber.

Using fabrication techniques such as chemical vapor deposition (CVD), it is possible to produce nanoscale structures and special metamaterials that have specific absorption properties in the terahertz region. These structures, especially when combined with graphene, can have exciting applications in material identification and biorecognition. With a standard lithography process, graphene can be fabricated and placed into special structures that can provide favorable THz responses to aqueous environments and biomolecules. Finally, measuring absorption values using THz time-domain spectroscopic systems allows researchers to obtain detailed information about the material content, its changes under different conditions, and the possible effects

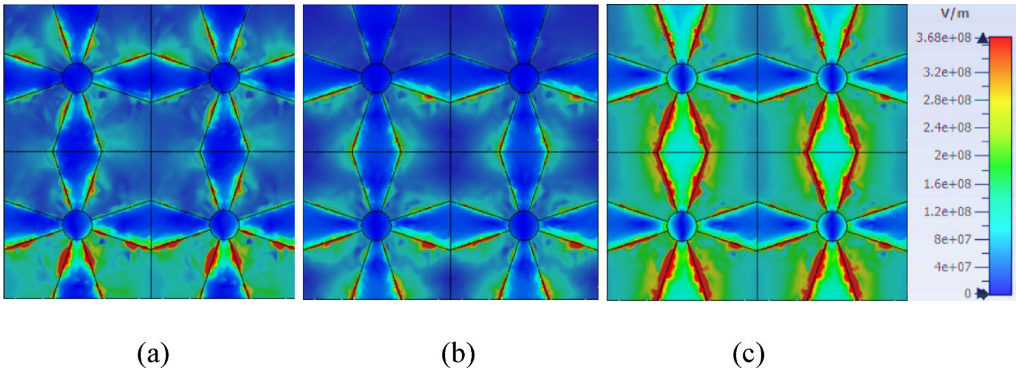

Fig. 9. Electric field [real (Ez)] distributions in the normal incidence of TE waves at frequencies of **(a)** 4.71 THz, **(b)** 7.43 THz, **(c)** 8.32THz.

of biological particles on optical properties. This type of analysis can help better understand materials' behavior in the terahertz region and lead to the development of new technologies and applications[31].

Figure 9 shows the electric field dispersion [real (Ez)] in the TE mode investigated at different frequencies. As shown in Fig. 9(a), at the frequency of 4.71 THz, there is a higher density field distribution at the upper and lower edges, which shows the first frequency peak band. Furthermore, Fig. 9(b) shows the field distribution at 7.43 THz, where the field shows a horizontal configuration with increasing density at the edges. Finally, Fig. 9(c) shows the field distribution at 8.32 terahertz, which again shows a lower density at the top and bottom edges due to its distance from the resonance peak frequency. These results show significant changes in electric field distribution with frequency change.

Conclusion

This study presents an ultra-high-sensitivity graphene-based terahertz biosensor featuring a novel radial pattern and multi-layer architecture for precise blood antigen detection. The proposed design achieves exceptional absorption rates exceeding 98% across targeted frequencies, ensuring robust and accurate analyte sensing. Testing with C_Hb analytes at concentrations ranging from 20 to 260 nanograms per milliliter revealed refractive index variations from 1.335859 to 1.398773, resulting in measurable absorption peak shifts that enable precise antigen detection. Among the three designed structures, the first configuration demonstrates the highest sensitivity of 10,514.1 GHz/RIU with a figure of merit (FoM) of 55.9, significantly surpassing previous designs. The second structure exhibits a sensitivity of 5,461.7 GHz/RIU with an FoM of 33.5, while the third achieves 2,390 GHz/RIU and an FoM of 13.8. Notably, the second structure maintains the highest sensitivity across all three absorption bands, offering a more consistent and linear response compared to the other two. These findings highlight the superior performance of the proposed biosensor in detecting blood antigens with remarkable sensitivity and precision. The integration of graphene and the novel radial-patterned architecture demonstrates its potential for next-generation terahertz biosensing applications, paving the way for advancements in medical diagnostics and early disease detection.

Data availability

The datasets used and/or analyzed during the current study available from the corresponding author on reasonable request.

Received: 6 March 2025; Accepted: 4 June 2025
Published online: 01 July 2025

References

1. Wu, J., Lin, X., Huang, X., Shen, Y. & Shan, P. F. Global, regional and National burden of endocrine, metabolic, blood and immune disorders 1990–2019: a systematic analysis of the global burden of disease study 2019. *Front. Endocrinol.* **14**, 1101627 (2023).
2. Altug, H., Oh, S. H., Maier, S. A. & Homola, J. Advances and applications of nanophotonic biosensors. *Nat. Nanotechnol.* **17** (1), 5–16 (2022).
3. Meixner, A. J., Fleischer, M., Kern, D. P., Sheremet, E. & McMillan, N. (eds) *Applications* (De Gruyter, 2022). https://doi.org/10.1515/9783110442908
4. Bhargava, M. *Evolution of Haematology in India: A Haematologist's Perspective*. Cambridge Scholars Publishing, Accessed: Jan. 12, 2025. [Online]. (2024). Available: https://books.google.com/books?hl=en&lr=&id=GEg4EQAAQBAJ&oi=fnd&pg=PR5&dq=Kumar,+S.,+Patel,+R.,+%26+Gupta,+A.+(2023).+Red+Blood+Cell+Diagnostics:+Challenges+and+Innovations.+Journal+of+Hematology+%26+Oncology,+16(2)&ots=F5NWQeopCn&sig=5FUtFpwmikzSiUscsXe0Ojunzcc
5. Newton, H. S. & Dobrovolskaia, M. A. Immunophenotyping: analytical approaches and role in preclinical development of nanomedicines. *Adv. Drug Deliv. Rev.* **185**, 114281 (2022).
6. Peña-Bahamonde, J., Nguyen, H. N., Fanourakis, S. K. & Rodrigues, D. F. Recent advances in graphene-based biosensor technology with applications in life sciences. *J. Nanobiotechnol.* **16** (1), 75. https://doi.org/10.1186/s12951-018-0400-z (Dec. 2018).
7. Teixeira-Santos, R., Belo, S., Vieira, R., Mergulhão, F. J. & Gomes, L. C. Graphene-Based composites for biomedical applications: surface modification for enhanced antimicrobial activity and biocompatibility. *Biomolecules* **13** (11), 1571 (2023).

8. Ghodrati, M. & Uniyal, A. Exploring Metasurface-Based biosensor: new frontiers in sensitivity and versatility for biomedical applications. *Plasmonics Nov*. https://doi.org/10.1007/s11468-024-02640-7 (2024).
9. Zhou, J., Wang, Y., Zhang, L. & Li, X. Plasmonic biosensing based on non-noble-metal materials. *Chin. Chem. Lett.* **29** (1), 54–60 (2018).
10. Madkour, L. H. *Carbon-Based Nanocomposite Applications and Microelectronic Technologies*. CRC Press, Accessed: Jan. 12, 2025. [Online]. (2024). Available: https://books.google.com/books?hl=en&lr=&id=j1gpEQAAQBAJ&oi=fnd&pg=PP1&dq=Real-Time+Monitoring+of+Red+Blood+Cells+Using+Graphene-LSPR+Biosensors.&ots=ZV6udVwPPf&sig=CDcapibYjYWBKkvHOxp1dDjxZMw
11. Reddy, Y. V. M. et al. Strategies, advances, and challenges associated with the use of graphene-based nanocomposites for electrochemical biosensors. *Adv. Colloid Interface Sci.* **304**, 102664 (2022).
12. Sengupta, J. & Hussain, C. M. Early detection of cancer utilizing biosensors based on 'green graphene': an innovative and sustainable methodology for advancing cancer diagnosis. *TrAC Trends Anal. Chemistry*, **167**, 117254, (2023).
13. Syama, S. & Mohanan, P. V. Comprehensive application of graphene: emphasis on biomedical concerns. *Nano-Micro Lett.* **11** (1, p. 6,). https://doi.org/10.1007/s40820-019-0237-5 (Dec. 2019).
14. Vdovin, E. E. et al. A magnetically-induced coulomb gap in graphene due to electron-electron interactions. *Commun. Phys.* **6** (1), 159 (2023).
15. Masoudian Saadabad, R., Huang, L., Evlyukhin, A. B. & Miroshnichenko, A. E. Multifaceted anapole: from physics to applications. *Opt. Mater. Express*. **12** (5), 1817–1837 (2022).
16. Esfandiari, M., Lv, X., Chamani, S. & Yang, Y. Graphene metasurfaces: advances in Lens applications, design strategies, and fabrication techniques. *Materials Today Electronics*, **11**, 100140, (2025).
17. Nasiri Shehni, P. & Mehranpour, M. Tunable THz multi-beam antenna sensor using graphene sheets. *Appl. Opt.* **64** (8), 2002–2008 (2025).
18. Farmani, A., Mir, A. & Sharifpour, Z. Broadly tunable and bidirectional Terahertz graphene plasmonic switch based on enhanced Goos-Hänchen effect. *Appl. Surf. Sci.* **453**, 358–364 (2018).
19. Rafighirani, Y., Javidan, J. & Heidarzadeh, H. Development of a Multi-Band High-Sensitivity Polarization-Independent absorber: A biosensor for simultaneous detection of multiple Cancer biomarkers. *Plasmonics*, **20**, 1–9, (2024).
20. Balanis, C. A. *Antenna Theory: Analysis and Design* (Wiley, 2015).
21. Khodaie, A. & Heidarzadeh, H. Split ring Resonator-Based multimode plasmonic optical biosensors for comprehensive antigen detection. *Sens. Imaging*. **25** (1), 63. https://doi.org/10.1007/s11220-024-00514-0 (Oct. 2024).
22. Khodadadi, B., Babaeinik, M., Ghods, V. & Rezaei, P. Triple-band metamaterial perfect absorber for refractive index sensing in THz frequency. *Opt. Quant. Electron.* **55** (5), 431. https://doi.org/10.1007/s11082-023-04684-1 (May 2023).
23. Manikandan, E., Karthigeyan, K. A., Arivarasi, A. & Papanasam, E. High-Q and FOM dual-band polarization dependent ultra-narrowband Terahertz metamaterial sensor. *IEEE Photonics J.* **15** (1), 1–6 (2023).
24. Liang, D. & Chen, T. Optical modulated graphene metamaterial based on plasmon-induced transparency in the Terahertz band: application for sensing. *Diam. Relat. Mater.* **131**, 109613 (2023).
25. Bahador, H. Five-segment THz refractive index metamaterial biosensor with perfect absorption for carcinoembryonic antigen measurement, *IEEE Sensors Journal*, Accessed: Jan. 02, 2025. [Online]. (2024). Available: https://ieeexplore.ieee.org/abstract/document/10597354/
26. Khodadadi, B., Rezaei, P. & Hadipour, S. Dual-band polarization-independent maze-shaped absorber based on graphene for Terahertz biomedical sensing. *Opt. Express*. **33** (3), 3869–3880 (2025).
27. Wekalao, J. et al. Terahertz plasmonic biosensor leveraging Ag-Au-Graphene heterostructures for quantitative hemoglobin analysis with machine learning algorithms for performance optimization. *Plasmonics Sep.* https://doi.org/10.1007/s11468-024-02520-0 (2024).
28. Khodadadi, B., Babaeinik, M., Ghods, V. & Rezaei, P. Sensitivity increment of metamaterial-based refractive index sensor with silicon layers. *Silicon* **15** (15), 6745–6759 (2023).
29. Norouzi-Razani, A. & Rezaei, P. Multiband polarization insensitive and tunable Terahertz metamaterial perfect absorber based on the heterogeneous structure of graphene. *Opt. Quant. Electron.* **54, 7, p. 407**, https://doi.org/10.1007/s11082-022-03813-6 (Jul. 2022).
30. Rezagholizadeh, E., Biabanifard, M. & Borzooei, S. Analytical design of tunable THz refractive index sensor for TE and TM modes using graphene disks. *J. Phys. D*. **53** (29), 295107 (2020).
31. Rafighirani, Y., Javidan, J. & Heidarzadeh, H. Polarization-independent tunable multi-band Terahertz absorber based on graphene structure to design the ultra-high sensitive biosensors. *Phys. Scr.* **99** (7), 075014 (2024).

Author contributions
All authors has same conterbition.

Declarations

Competing interests
The authors declare no competing interests.

Additional information
Correspondence and requests for materials should be addressed to H.H.

Reprints and permissions information is available at www.nature.com/reprints.

Publisher's note Springer Nature remains neutral with regard to jurisdictional claims in published maps and institutional affiliations.